

First Principles Calculations of the Adsorption of NH₃ on a Periodic Model of the Silica Surface

Bartolomeo Civalleri and Piero Ugliengo*

Dipartimento di Chimica IFM, Università di Torino, Via P. Giuria, 7, 10125 Torino, Italy

Received: June 30, 2000

For the first time, the interaction of a NH₃ molecule with a periodic hydroxylated surface resulting from the (100) face of edingtonite has been studied ab initio by both the Hartree–Fock and B3-LYP levels using a localized Gaussian basis set and the fully periodic treatment as coded in the CRYSTAL98 program. For comparison, molecular clusters of different size and topology have also been adopted. The simulation mimics the physical adsorption of NH₃ on a highly dehydroxylated amorphous silica surface, that being the OH density of the adopted (100) edingtonite face around 2 OH/nm². Geometries, binding energy, and the vibrational frequency of the surface OH groups perturbed by NH₃ have been fully characterized. The basis-set dependence of the binding energy has also been addressed using basis sets for the periodic calculation that include both diffuse functions and multiple sets of polarization functions. BSSE and thermal corrections to the binding energy have also been included. Our best estimate of the $\Delta H^0(0)$ is -31.2 ± 0.6 kJ/mol for the periodic model, to be compared with the experimental molar heat of adsorption of about -45 kJ/mol and with the isosteric heat of adsorption of about -37 kJ/mol. The anharmonic frequency shift $\Delta\omega_{01}$ caused by NH₃ adsorption on the OH stretching mode has been computed to be -663 cm⁻¹, including estimated corrections for basis set and B3-LYP deficiencies, mechanical coupling, and BSSE. The comparison with the value of -950 cm⁻¹ measured at 4 K on amorphous silica shows a definite underestimation, in agreement with the too-high computed $\Delta H^0(0)$. It is concluded that the proposed periodic edingtonite slab behaves satisfactorily as a model for the dehydroxylated surface of siliceous materials, also requiring very few computer resources. Cagelike clusters, when properly designed, give results that are close to those obtained with the periodic model. The remaining differences between the computed properties are due to cooperative interactions of a long-range nature that are not accounted for by the finite cluster.

1. Introduction

Detailed information concerning the structure of amorphous silica is lacking because of its nature as a random network of corner-sharing rigid SiO₄ tetrahedra linked to one another by siloxane bridges.^{1,2} The extreme flexibility of the Si–O–Si angle is the reason behind the great structural variability of siliceous-based materials, ranging from dense crystalline forms such as quartz, to a large variety of microporous zeolites, to a large collection of amorphous silicas. Whereas microporous crystalline silicas are the ideal framework in which to run heterogeneous catalytic reactions, amorphous silicas are of paramount relevance for chromatography, adsorption, and metal-supported catalysis.³

Details of the bulk structure of amorphous silica come from both experiment⁴ and computer simulations.⁵ However, the corresponding knowledge of the sites at the external surface is by far more scarce.^{6,7} Ideally, the Si atoms at the external surface become tricoordinated; however, because of the ubiquitous presence of water in the environment, hydroxyl groups act as capping groups to saturate the unfilled Si valence. Figure 1 shows an image of an idealized grain of amorphous silica and its surface sites, namely isolated silanol, vicinal, geminal, and silanol groups, interacting by H-bond.⁸ The isolated silanol consists of one OH group bonded to a Si atom and not interacting with other isolated sites. The geminal site has two OH groups per Si atom; because of their geometrical features, they are not mutually H-bonded. The vicinal site is made by

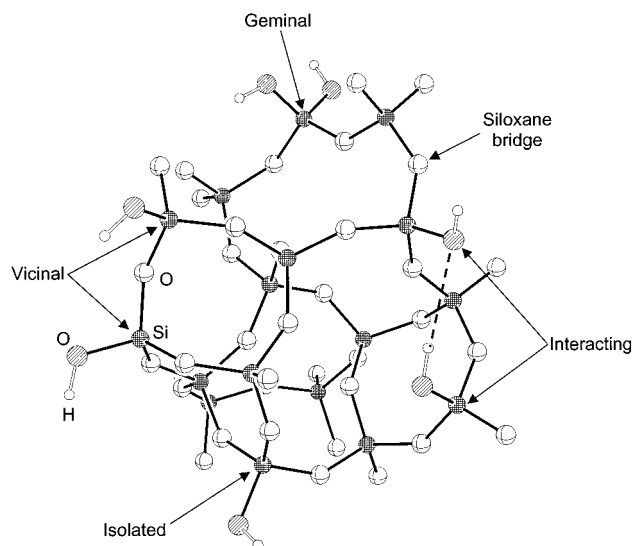


Figure 1. Pictorial view of a hypothetical amorphous silica grain. Highlighted are all possible sites at the surface.

two SiOH groups separated by one siloxane bridge; as for geminals, geometrical constraints do not allow the formation of an internal H-bond. To allow for H-bonding in SiOH groups, more than one Si–O–Si bridge is required as is the case for interacting silanols. The concentration and distribution of these sites is a function of both sample preparation and thermal

treatments. At high treatment temperature, both vicinal and interacting silanols condense, giving rise to a siloxane bridge and a water molecule. If this is the case, only isolated and geminal sites remain, surrounded by siloxane bridges.

It was established long ago⁹ that the concentration of isolated silanols for a highly dehydrated amorphous silica is between one and two OH groups per nm² and that only a small concentration of geminal sites remains in this condition. Each silanol is now spatially isolated from its next neighbors. Because of the chemical nature of the silanol groups, their vibrational properties can be easily studied by infrared spectroscopy. On highly dehydrated surfaces, a single, well-defined band due to the OH stretch is measured at about 3742 cm⁻¹ on an otherwise featureless spectral region extending from 3730 to 2000 cm⁻¹.⁹ This ease of study also allows us to track the perturbations of the OH stretching frequency upon adsorption of molecules from the gas phase. In that respect, it is now well-established that H-bonding interactions are a significant fraction of the forces between these OH groups and the ad-molecules.¹⁰ The remaining component of the interaction energy is due to the dispersive contribution which becomes dominant for large unpolar organic molecules. The interplay between these forces is such that different molecules become selectively adsorbed on amorphous silica, which is, for this reason, largely adopted as an active support in chromatography and adsorption processes.

To understand the microscopic steps involved in the recognition between the surface OH groups and the ad-molecule, not only IR but also NMR¹⁰⁻¹² and microcalorimetric measurements¹³ have been traditionally employed. More recently, computer modeling based on ab initio techniques has also been used.¹⁴

In such quantum mechanical studies, the interaction of molecules with the infinite surface has been modeled by a cluster approach, i.e., a finite number of atoms inclusive of the active site are cut out from the surface.¹⁵ Dangling bonds are saturated with some arbitrary atoms or atomic groups, such as H, F, or OH. The resulting cluster is now a molecule that can be treated by the standard molecular ab initio programs. However, only local effects are considered, whereas long-range effects on the electrical properties of the active site are completely neglected. Furthermore, the size of the cluster also has to be decided.

To avoid those problems, a periodic treatment is desirable: an infinite replica of the active site is carried out and an ab initio program able to exploit the crystalline nature of the material is adopted. Because of the replica, lateral interactions between the adsorbate molecules should also be taken into account when computing the adsorption energy. The imposed periodicity obviously restricts the study to crystalline materials only.

On the other hand, the ab initio treatment of the surface of an extended amorphous silica has never been tackled. This is obviously because of the lack of detailed structural information about the active sites and the need to ensure that a large enough portion of the material, such as the main features of the active sites, is properly taken into account. One possibility is to design a sufficiently large unit cell in which the structural features of the amorphous material are properly included and treat the computational problem using a periodic quantum mechanical code. This has recently been done, as far as the bulk vitreous SiO₂ structural features are concerned, by ab initio molecular dynamics techniques,¹⁶ but no similar calculations have been performed to simulate the surface sites. Although they may be

elegant and appealing, the ab initio molecular dynamics calculations are also extremely demanding in terms of computer resources.

A different approach, and one that has been followed in the present paper, is to design a crystalline model of silica that has structural and vibrational features close enough to those measured for the amorphous silica surface. To this aim, we have recently studied¹⁷ the electronic, structural, and vibrational properties of the (100) hydroxylated face cut from the bulk edingtonite using a periodic quantum mechanical approach based on localized Gaussian basis functions. The considered films (of variable thickness) have regular arrays of hydroxyl groups and are an idealized structural model for crystalline siliceous materials. Moreover, because of the resulting OH density at the surface, the (100) face of edingtonite may also be considered as a model system of a highly dehydrated amorphous silica surface. A number of attractive properties make it suitable for the simulation of silica surfaces: (1) The surface energy of the (100) face is low, with no reconstruction or relaxation. (2) The unit cell contains only five SiO₂ groups, implying a modest computational effort. (3) The density of surface hydroxyls is close to that experimentally observed on dehydrated silica. (4) The stretching frequency of the surface OH group at the surface is very close to that computed with the largest cagelike clusters, and also to the experimental value for isolated hydroxyls on amorphous silica.

In this paper we extend our previous work adopting the same periodic approach for simulating the adsorption of NH₃ on the (100) hydroxylated face of edingtonite. As far as we know, this is the first periodic ab initio attempt at both HF and B3-LYP levels to model the interaction of NH₃ with a hydroxylated silica surface model. Data for the periodic model are also supplemented with those from a pure cluster approach on well-designed, cagelike silica clusters already studied in the past.¹⁸

2. Models

In the present study, we take as reference the results obtained in ref 17 and we adopt the same models. For sake of clarity, we also keep the same notation as in ref 17. We cut out a slab from bulk edingtonite (EDI)¹⁹ parallel to the (100) face, and labeled it as EDL x S n , x indicating the direction perpendicular to the surface, S standing for slab, and n indicating the number of 4-1 chain (see ref 17 for details) layers perpendicular to the slab. Here, all the calculations were done by adopting the simplest model, i.e., EDL x S1, because we have shown¹⁷ that results for the double-slab EDL x S2 are indistinguishable from those for EDL x S1.

Two cluster models are also considered: the simple silanol molecule H₃SiOH (SIL), and a cagelike cluster model. The former is the simplest cluster for modeling isolated hydroxyl groups in silica, and is the subject of many papers.²⁰⁻²⁴ The latter is a recently proposed cagelike model,¹⁸ H₇Si₅O₆(OH), hereafter referred to as A.²⁵ The reason for considering the A cluster lies in its particular topology, as the building block of the 4-1 chain of the EDL x S1.¹⁷ All dangling bonds have been saturated with hydrogen atoms except the OH group that mimics the active site. The adopted models, in interaction with ammonia, are shown in Figure 2.

3. Computational Methods

All calculations have been carried out with the Hartree-Fock (HF) method and the density functional theory (DFT) B3-LYP hybrid method with Becke's²⁶ exchange functional and the Lee, Yang, and Parr²⁷ correlation functional. Cluster model calcula-

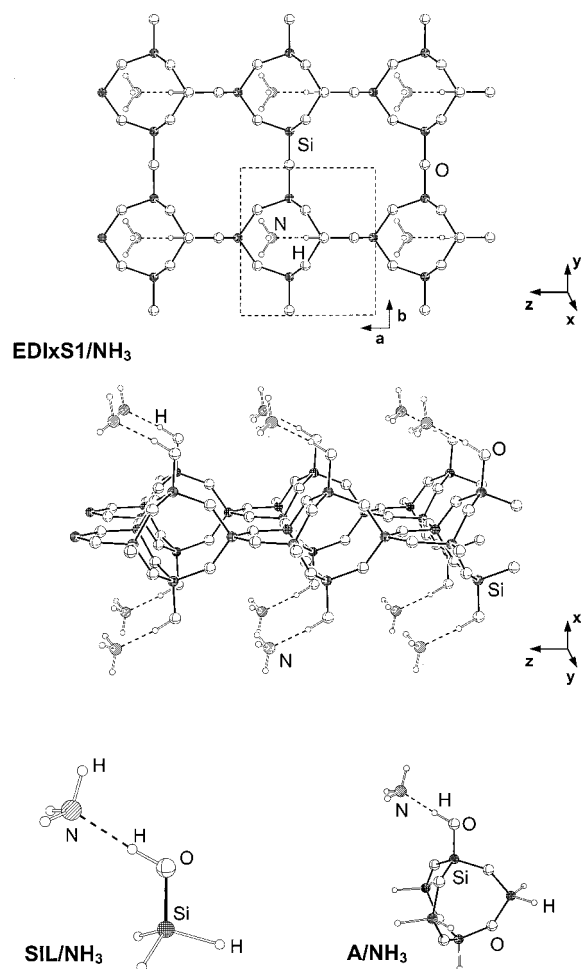


Figure 2. Structure of the periodic model EDLxS1 and of the two cluster models, SIL and A, interacting with ammonia.

tions were performed by means of Gaussian98,²⁸ while periodic calculations were carried out by the use of CRYSTAL98.^{29,30}

The geometries of the cluster models, both alone and interacting with NH₃, were fully optimized using analytical gradient techniques imposing a C_s symmetry. The slab geometry was optimized following the procedure adopted in our previous paper.¹⁷ The slab alone was optimized with the GULP code,^{31,32} using the parameters designed by Schröder and Sauer³³ and by Sierka and Sauer³⁴ with reference to the HF and B3-LYP computations, respectively: starting from the resulting optimized geometries (hereafter referred to as GHF and GB3 for HF and B3-LYP optimizations, respectively), the OH group was reoptimized only at the corresponding full HF and B3-LYP ab initio levels. For the case of the slab interacting with NH₃, all atoms were kept fixed at the GHF or GB3 optimum, whereas the OH group and the NH₃ molecule were optimized by means of a numerical gradient technique³⁵ at full HF and B3-LYP levels. During the optimization, both the slab cell and the symmetry were kept fixed. To keep as many symmetry operators as possible, the interacting molecule was adsorbed onto both sides of the slab. All periodic calculations have been carried out by using a shrinking factor $S = 2$, corresponding to four k -points in the Brillouin zone at which the Hamiltonian matrix has been diagonalized. The distance between NH₃ molecules at the opposite sides of the slab is large enough to ensure a negligible mutual effect. Geometry optimizations were carried out adopting a modified 6-21G(d) basis set for Si and a modified 6-31G(d) basis set for O, as reported in ref 35, as well as a 3-1G(p) for H and a standard 6-31G(d) for N.

For both periodic and cluster models, single-point calculations on optimized geometries were done with larger basis sets at the B3-LYP level only. In a first step, the basis set of the framework Si, O, and H atoms was not changed, whereas for the OH \cdots NH₃ moiety, the following standard basis sets were employed: 6-31+G(d,p), 6-31+G(2d,2p), 6-31++G(2d,2p), 6-311+G(2d,2p), and 6-311++G(2d,2p). In a final step, single-point calculations were also carried out with two different basis sets for the framework atoms: a 6-31G(d) for both Si and O, and as will be discussed later, an 88-311G(d) basis set for Si and an 8-411G(d) basis set for O,³⁶ both combined with a 6-311+G(2d,2p) for the OH \cdots NH₃ moiety.

The computed binding energies were corrected for the basis set superposition error (BSSE) by the use of the full counterpoise method³⁷ as implemented in Gaussian98 and in CRYSTAL98 for cluster and periodic cases, respectively.

For all considered systems, in agreement with previous works,^{21–23} the anharmonic OH stretching frequency was computed numerically. The O–H distance was considered as a normal mode decoupled with respect to all other modes. The OH bond length was then varied around the equilibrium value, and the potential energy was evaluated at 26 different points. The energy values were best-fitted with a sixth-order polynomial. The resulting monodimensional nuclear Schrödinger equation was solved by following a numerical algorithm proposed in ref 38, by means of the program ANHARM.³⁹ The same procedure described for the free slab was used for the interaction with NH₃, freezing the O \cdots N distance at the optimum value during the O–H scan. For such calculations, only the basis set adopted for optimizing the geometry of the studied systems was used.

4. Results and Discussion

4.1. Geometries of the Adducts. Optimized structures of cluster models and the EDLxS1 slab interacting with NH₃ are shown in Figure 2, and the main structural features of the studied systems are summarized in Table 1.

The SiO bond length decreases significantly from SIL to EDLxS1, whereas the OH bond length is almost unchanged among the considered models. The intermolecular H \cdots N distance shows a behavior along the series SIL, A, EDLxS1 that depends on the adopted computational level. At the HF level, a monotonic decrease of the H \cdots N distance is computed, at variance with the results obtained at the B3-LYP level. In the latter case, the H \cdots N distance increases along the series A, SIL, and EDLxS1. This point will be further addressed in the subsequent section. In general, it is a well-known fact that B3-LYP gives longer OH bond lengths and shorter intermolecular H \cdots N distances with respect to HF, in agreement with what is known about H-bonding interactions at the molecular level.⁴⁰

The values of the intermolecular angles $\angle\text{O–H}\cdots\text{N}$ and $\angle\text{H}\cdots\text{N–H}$ (the N–H bond being in the Si–OH plane) give insight into the localization of NH₃ with respect to the adsorbent site. The variations of these angles are a measure of the different electric fields suffered by NH₃ in the region close to the adsorbent OH group. Results for the two clusters SIL and A at both the HF and the B3-LYP levels show a very good internal consistency, the $\angle\text{O–H}\cdots\text{N}$ angle being close to 180°, as expected, in all cases. The average $\angle\text{H}\cdots\text{N–H}$ angle is around 107° and 109° at the HF and B3-LYP levels, respectively, with a variance less than 1°. When considering the results for EDLxS1, we noted significant differences, as reported in Table 1. At the HF level, the angle $\angle\text{H}\cdots\text{N–H}$ decreases by about 7° with respect to the average values computed for the clusters, i.e.,

TABLE 1: Main Geometrical Features of SIL/NH₃, A/NH₃, and EDLxS1/NH₃ Structures. (ΔE , ΔE^C , and $\Delta H^0(0)$ are, respectively, the binding energy, the one corrected for BSSE, and the heat of formation at 0 K)^a

model	Si–O	O–H	H···N	\angle O–H···N	\angle H···N–H	ΔE	ΔE^C	$-\Delta H^0(0)$
				HF				
SIL/NH ₃	1.624	0.955	1.998	179.7	106.4	34.7	31.0	22.3
A/NH ₃	1.595	0.957	1.945	179.9	108.7	38.3	34.1	25.4
EDLxS1/NH ₃	1.602	0.959	1.921	179.9	99.6	40.0	35.3	26.6
				B3-LYP				
SIL/NH ₃	1.640	0.988	1.826	179.1	108.6	47.2	40.6	31.6
A/NH ₃	1.608	0.994	1.771	179.4	111.6	52.5	45.2	36.5
EDLxS1/NH ₃	1.604	0.993	1.836	174.2	125.0	59.1	50.1	41.4
expt ^b								37
expt ^c								25/60

^a Energies in kJ/mol; bond length, in Å, and bond angles, in degrees. Basis set: Si[6-21G(d)]; H,O,N[6-31G(d,p)]. ^b From a set of isotherms at different temperature (ref 41). ^c Microcalorimetric measurements at 300 K (ref 13). Higher value in the limit of zero coverages; lower value for higher coverages.

the whole NH₃ is rotating anticlockwise around the y axis (see Figure 2 for the adopted gauge) to increase the distance between its two H atoms and the basal plane of the EDI slab. The opposite behavior is seen at the B3-LYP level, in which a clockwise rotation of about 15° brings the two H atoms of NH₃ toward the EDI framework. A possible interpretation is based on a weak attractive interaction between the oxygen of the nearby OH group and the slightly acidic hydrogens of NH₃. This fact is, however, accounted for only at the B3-LYP level, and it is in line with the sizable increment of the H···N distance for the EDLxS1/NH₃ structure when compared with the value computed for the A/NH₃ adduct. Even if such changes in the intermolecular part are small, they may influence both the binding energy and the OH stretching frequency, as we will show in the following sections.

4.2. Binding Energies. In a periodic treatment of surface adsorption phenomena, the binding energy per unit cell per adsorbate molecule is defined as

$$\Delta E = E(\text{slab}) + E(\text{ads}) - E(\text{slab/ads}) \quad (1)$$

where $E(\text{slab/ads})$ is the total energy of the slab in interaction with the periodic array of adsorbed molecules, $E(\text{slab})$ is the energy of the slab alone, and $E(\text{ads})$ is the energy of the periodic array of adsorbed molecules without the underneath solid surface. All these quantities are defined per unit cell and are negative.

However, the observed binding energy, ΔE_{exp} , corresponds to the process in which the molecules move from an ideal gas state onto the surface, and is defined as

$$\Delta E_{\text{exp}} = E(\text{slab}) + N \cdot E(\text{mol}) - E(\text{slab/ads}) \quad (2)$$

where $E(\text{mol})$ is the energy of one isolated adsorbate molecule and N is the number of adsorbed molecules per unit cell. The difference between the computed ΔE and the experimental ΔE_{exp} is due to the interaction energy, per unit cell, between the adsorbate molecules themselves, i.e., without the underneath surface:

$$\Delta E_{\text{exp}} - \Delta E = \Delta E_L = E(\text{ads}) - N \cdot E(\text{mol}) \quad (3)$$

ΔE_L is also known as the *lateral interaction energy* and can be either positive (repulsion) or negative (attraction) depending on the nature of the ad-molecules. In the limit of very low coverages, i.e., large distances between the adsorbate molecules, ΔE_L will obviously tend toward zero, so that $\Delta E_{\text{exp}} \approx \Delta E$.

In intermolecular interactions, the computed binding energy should always be corrected for the BSSE following the counterpoise method proposed for molecular complexes. There-

fore, the BSSE corrected binding energy ΔE^C becomes

$$\Delta E^C = E(\text{slab/[ads]}) + E([\text{slab}]/\text{ads}) - E(\text{slab/ads}) \quad (4)$$

in which $E(\text{slab/[ads]})$ and $E([\text{slab}]/\text{ads})$ are, respectively, the energy of the slab with the basis functions of the adsorbate only, and vice versa.

Table 1 shows the HF and B3-LYP computed binding energies, calculated with the same basis set adopted for the geometry optimization. We have computed the lateral interaction energy and found it to be negligible (around 1% of ΔE), so the reported ΔE are calculated with respect to the isolated NH₃.

As previously pointed out,¹⁸ binding energies computed for the minimal cluster model, SIL, are significantly lower than those computed for the cage model. This could be easily explained considering the different polarization effects induced on the silanol group by the oxygen atoms of the first coordination shell of the silicon atom of the A cluster. These effects yield an enhancement of the acidity in the cagelike model and a subsequent higher binding energy. For the periodic model, the polarization and long-range effects are such that both the HF and the B3-LYP methods give a higher binding energy than the cage cluster A. It is worth noting that the inclusion of long-range interactions, which are absent in the cluster models, is not the only reason for the higher ΔE values. The structural effects are also relevant, as will be discussed later on.

The inclusion of electron correlation yields an important contribution to the binding energies, the B3-LYP results being about 30 to 50% higher than the corresponding HF ones. The increase of ΔE when passing from cluster A to the EDLxS1 is also significantly higher at B3-LYP than at the HF level (2 and 6 kJ/mol, respectively).

Molar heats of adsorption have been measured in the past on highly dehydroxylated amorphous silica samples. Hertl and Hair long ago⁴¹ reported an isosteric heat of about −37 kJ/mol. Fubini et al.¹³ measured, by direct microcalorimetry, values of the differential heat of adsorption, ranging from −60 to −25 kJ/mol for low and high coverages, respectively. This range in the differential heat of adsorption may be due to the structural heterogeneity of the isolated silanols at the silica surface, or to multiple interactions resulting from the clustering of NH₃ molecules at the hydroxyl groups. In that respect, values in the low coverage regime are less affected by the last process, so that values around −60/−40 kJ/mol can be assumed as a reference to be compared with the computed heats of formation. Furthermore, the molar heat of adsorption measured at 40 torr¹³ of equilibrium pressure is around −45 kJ/mol, in reasonable agreement with the isosteric heat measured by Hertl and Hair.⁴¹ To allow for a direct comparison with the experimental heats

TABLE 2: Dependence of the B3-LYP Binding Energies ΔE and ΔE^C on the Quality of the Basis Set^a

basis set ^b	NAO ^d	SiL/NH ₃		A/NH ₃		EDLxS1/NH ₃	
		ΔE	ΔE^C	ΔE	ΔE^C	ΔE	ΔE^C
6-31G(d,p)	0	47.2	40.6	52.5	45.2	59.1	50.1
6-31+G(d,p)	16	41.3	34.0	47.0	36.6	53.6	44.1
6-31+G(2d,2p)	60	34.9	30.6	40.4	33.2	47.4	40.2
6-31++G(2d,2p)	68	35.3	30.7	40.8	33.3	50.6	40.6
6-311+G(2d,2p)	84	33.5	30.1	38.8	32.6	46.2	39.0
6-311++G(2d,2p)	92	33.8	30.2	38.7	32.1	49.3	39.5
basis set ^c							
6-21G(d)	84	33.5	30.1	38.8	32.6	46.2	39.0
6-31G(d)	84	33.6	30.3	38.3	33.6	44.7	39.7
Nada et al. ^e	120	34.3	30.7	38.4	34.1	44.7	40.6
$\langle \Delta E \rangle^f$		34.2	30.4	39.2	33.2	47.2	39.9
σ		0.7	0.3	1.1	0.7	2.4	0.6
$\langle \Delta H^0(0) \rangle^f$			21.4		24.5		31.2
σ			0.3		0.7		0.6

^a Energies in kJ/mol. ^b OH group and NH₃ basis set; framework atoms basis set: Si[6-21G(d)], O,H[6-31G(d,p)]. ^c Framework atoms basis set; OH group and NH₃ basis set: 6-311+G(2d,2p). ^d Relative number of AO basis functions with respect to the 6-31G(d,p) basis set. ^e Si[88-31(d)], O[8-411(d)] (ref 36). ^f Computed excluding the first two rows.

of adsorption, the computed binding energies ΔE must be corrected for the BSSE, the zero-point vibrational energy (ZPE), and, finally, by the thermal corrections at the temperature of the experimental measurements. Because the last contribution is small at room temperature, only the ZPE correction was taken into account so that the heat of adsorption at 0 K, $\Delta H^0(0)$ could be computed and compared with the experimental data. For evaluating the ZPE, the whole set of frequencies is needed. Such a calculation is routinely feasible for molecular systems (SiL and A) at variance with the periodic calculations on EDLxS1, because the second derivatives of the total energy are not available in CRYSTAL98. In the latter case, we have assumed that the ZPE correction for EDLxS1 is the same as that computed for cluster A.

It is worthy of note that the BSSE is higher for the periodic case than for the cluster models and that the BSSE at B3-LYP is larger than the corresponding value at HF, as was previously found for hydrogen-bonded molecular systems.⁴⁰ The BSSE is sizable and cannot be ignored, being of the same order of magnitude as the electron correlation contribution (11 and 14% of ΔE at HF and B3-LYP, respectively).

When both the BSSE and the ZPE are taken into account, it is possible to correct the ΔE to arrive at the final $\Delta H^0(0)$ (see Table 1). The HF $\Delta H^0(0)$ values are definitely underestimated for all considered models, whereas B3-LYP gives results in better agreement with the experimental data, the $\Delta H^0(0)$ value for EDLxS1 being -41.4 kJ/mol. The corresponding values for the cluster models are -36.5 and -31.6 kJ/mol for A and SiL, respectively, highlighting the close correspondence between the results for EDLxS1 and the cage A.

A more convincing estimate of $\Delta H^0(0)$ should include the basis-set dependence of the computed data. It is expected that improving the quality of the basis set will decrease both the ΔE and the BSSE, so that a better estimate of $\Delta H^0(0)$ can be computed. In the next section, the basis-set dependence of the computed ΔE will be extensively discussed.

4.2.1. Basis-Set Effects on Binding Energies. For weak molecular complexes, calculations with large and polarized basis sets with very diffuse outer exponents are usually adopted to improve the computed ΔE . Unfortunately, the same procedure cannot be adopted as such for periodic calculations, because of the linear dependence of the basis set. To cure the problem, contraction of the outer exponents has also been suggested.²⁹ We followed two different strategies to overcome the problem.

First, the basis set of the framework atoms of the slab (Si[6-21G(d)], O[6-31G(d)]) and that of the hydrogen atoms belonging to the cluster (H[3-1G(p)]) were kept unchanged, whereas only the basis set of the OH \cdots NH₃ moiety has been systematically improved. Pople's molecular basis sets of increasing quality have been adopted (see Table 2 for details). As a further step, the 6-311+G(2d,2p) basis set was fixed for the OH \cdots NH₃ moiety, whereas the basis set of the framework atoms was improved as much as allowed by the former limits (see Computational Methods section).

Calculations were carried out as single-point energy evaluations at the geometries previously optimized with the smaller basis set (see section 4.1). This is similar to the standard procedure adopted for molecular calculations, which is extended here to the case of periodic calculations.

Because the HF ΔE values were already underestimated, the basis-set effects on ΔE were limited to the B3-LYP case. The results are reported in Table 2.

As the data in Table 2 shows, the inclusion of diffuse functions on heavy atoms causes a dramatic decrease in the binding energy for both clusters and periodic calculations, in agreement with previous findings for hydrogen-bonded adducts within the DFT approach.⁴² When a second set of polarization functions is added, a further decrease in both ΔE and BSSE is seen. The improvement of the valence region (from 6-31G to 6-311G) does not bring any significant change in the ΔE values (less than 1 kJ/mol), as it does the addition of a set of diffuse *p* functions on hydrogen atoms. Results for the periodic calculations are more sensitive to the adopted basis sets, and ΔE values are also affected by a larger BSSE when compared to the cluster calculations.

To further reduce the BSSE, we improve the basis set of the framework atoms, as well. In a previous work concerning the rare gas/zeolite interactions modeled with CRYSTAL, Nada et al.³⁶ have already reported the sizable BSSE affecting the ΔE value computed with the 6-21G(d) basis set. To improve the results, they derived two new basis sets, namely an 8-411G(d) for O and an 88-31G for Si. These basis sets yield a better description of core states and are less affected by the BSSE. Results computed with Nada's basis set for the framework atoms and with 6-311+G(2d,2p) for the OH \cdots NH₃ moiety are included in the lower half of Table 2. As anticipated, there is a significant reduction of the BSSE, whereas the ΔE values are close to those obtained with the 6-31G(d) basis set for the framework atoms.

TABLE 3: Computed OH Stretching Frequency Shifts^a

	$\Delta\omega_{01}(\text{OH})$	$\Delta\omega_{02}(\text{OH})$	$\Delta\omega_e(\text{OH})$	$\Delta\omega_{e\kappa_e}(\text{OH})$
HF				
SIL/NH ₃	-335	-750	-253	41
A/NH ₃	-432	-980	-318	57
EDLxS1/NH ₃	-427	-985	-314	56
B3-LYP				
SIL/NH ₃	-614	-1361	-479	67
A/NH ₃	-792	-1766	-611	91
EDLxS1/NH ₃	-733	-1621	-575	78
expt ^b	-950			

^a Basis set: Si[6-21G(d)]; H₂O,N[6-31G(d)]. $\Delta\omega_{01}(\text{OH})$: fundamental frequency shift; $\Delta\omega_{02}(\text{OH})$: first overtone frequency shift; $\Delta\omega_e(\text{OH})$: harmonic frequency shift; $\Delta\omega_{e\kappa_e}(\text{OH})$: anharmonicity constant shift; all data in cm⁻¹. ^b IR spectroscopy at 4 K (ref 50).

With this combination of basis sets, the BSSE for the periodic calculations is close to that computed for the clusters.

As expected, the ΔE^C values are far less spread than the corresponding uncorrected ΔE values, the ΔE^C being around 40 kJ/mol already with the 6-31+G(2d,2p) basis set. We do not claim that the range of the adopted basis set will allow for any extrapolated ΔE value. However, to facilitate the discussion, the average ΔE^C has also been reported in the lower half of Table 2. Results for the periodic calculations show a larger dependence on the basis set for ΔE with respect to the ΔE^C values, being in the last case the standard deviation less 1 kJ/mol. By accounting for the ZPE contribution, we arrived at a final estimate of the B3-LYP $\Delta H(0)^0$: -21.2 ± 0.3 for SIL/NH₃, -24.5 ± 0.7 for A/NH₃, and -31.2 ± 0.6 for EDLxS1/NH₃, respectively. In summary, when reference to experimental molar heat of adsorption is addressed, it results that the computed $\Delta H(0)$ is definitely underestimated, with data for EDLxS1 being in better agreement with respect to values computed with the cluster approach. It is interesting to note that a similar behavior has been reported by Brändle and Sauer⁴³ for the computed $\Delta H^0(0)$ of ammonia adsorbed in a variety of microporous materials. Their simulations, based on a quite accurate embedded cluster approach, give results for the heat of adsorption which are also underestimated with respect to experimental values, even if less critically than the present data for silica. On the other hand, the spread in the experimental heats of formation is still large because of the different techniques adopted (both calorimetry and TPD), so no tight comparison is possible.

4.3. Vibrational Features. It is a well-known fact that the stretching frequency of the proton donor shifts to a lower wavenumber with respect to its free value because of the hydrogen-bond formation.⁴⁴ This phenomenon can be easily detected by means of IR spectroscopy and can also be computed with reasonable accuracy by ab initio methods. In the latter case, a harmonic approximation is usually adopted. However, as previously pointed out by some of us,^{40,45} and very recently by Silvi et al.,⁴⁶ Sauer et al.,^{47,48} and Jeanvoine et al.,⁴⁹ the introduction of anharmonic treatment is essential to reach a better agreement between computed and experimental data. This fact appears obvious when we consider that anharmonicity of the OH bond is quite sizable, at around 90 cm⁻¹.

Adopting the same procedure used in our previous paper on the slab alone,¹⁷ we have computed the OH stretching frequency for the system interacting with NH₃ and the corresponding frequency shift. The computed harmonic $\Delta\omega_e(\text{OH})$ and anharmonic $\Delta\omega_{01}(\text{OH})$ stretching frequency shifts for the adducts are reported in Table 3. The values have been computed with the same basis set used for the structure optimization.

TABLE 4: Dependence of the OH Stretching Frequency Shift for the SIL/NH₃ System on the Adopted Basis Set, Computational Level, and Mechanical Coupling^a

SIL/NH ₃	$\Delta\omega_{01}(\text{OH})$	$\Delta\omega_e(\text{OH})$	$\Delta\omega_h(\text{OH})$	μ
B3-LYP/S	-614	-479	-496	-27
B3-LYP/L	-571	-429	-452	-23
MP2/L	-549	-400	-422	-22
$\delta^{\text{B3-LYP}}(L-S)$	+43	+50	+44	
$\epsilon_L(\text{MP2-B3-LYP})$	+22	+29	+30	

^a S: framework basis set Si[6-21G(d)]; H₂O,N[6-31G(d)]. L: aug-cc-pVDZ basis set. $\delta^{\text{B3-LYP}}(L-S) = \Delta\omega(\text{B3-LYP/L}) - \Delta\omega(\text{B3-LYP/S})$; $\epsilon_L(\text{MP2-B3-LYP}) = \Delta\omega(\text{MP2/L}) - \Delta\omega(\text{B3-LYP/S})$; $\mu = \Delta\omega_h - \Delta\omega_e$.

The computed OH frequency shifts for the minimal cluster SIL are the smallest. This is a well-known finding⁴⁵ which is related to the too-less-acidic nature of SIL. The A cluster gives larger shifts, in agreement with our previous work on cage cluster models.¹⁸ However, quite unexpectedly, both the HF and the B3-LYP methods give values of $\Delta\omega_{01}(\text{OH})$ for A/NH₃ which are larger than those computed for the EDLxS1/NH₃ case. This result is surprising because both HF and B3-LYP ΔE s are higher for the periodic EDLxS1 case when compared to cluster results. In this respect, B3-LYP data shows the largest difference, the $\Delta\omega_{01}(\text{OH})$ values being -792 cm⁻¹ and -733 cm⁻¹ for A and EDLxS1, respectively.

IR spectra have been recorded on dehydrated amorphous silica samples in interaction with an NH₃ molecule at 300⁹ and 4 K,⁵⁰ respectively, giving rise to OH vibrational shifts of -650 cm⁻¹ and -950 cm⁻¹. The latter value is the one that can be compared with our computed values, because the quantum mechanical calculation mimics a configuration independent of the temperature. For all considered models, the HF shifts are definitely underestimated, in agreement with the too-low binding energies. However, even if B3-LYP data are in better agreement with the experiment, they are still underestimated. To allow for a more stringent comparison of the computed $\Delta\omega_{01}(\text{OH})$ shift with the experimental datum of -950 cm⁻¹, four effects should be considered: (1) the basis-set dependence; (2) the role of the BSSE; (3) the mechanical coupling of the OH mode with the remaining modes; and (4) the accuracy of the B3-LYP methods for computing hydrogen-donor vibrational shifts for H-bonded complexes.

To address the above points, we have used the simplest cluster, SIL/NH₃ (see Table 4 for details), in which basis-set dependence (from $S = 6-31G(d,p)$ to $L = \text{aug-cc-pVDZ}$), deficiencies in the electron correlation treatment (from the B3-LYP to the MP2 level), and mechanical coupling (from $\Delta\omega_h$ to $\Delta\omega_{01}$) are taken into account. The effect of the basis-set improvement is given by $\delta^{\text{B3-LYP}}(L-S) = \Delta\omega(L) - \Delta\omega(S)$, which shows that the B3-LYP values of $\Delta\omega_{01}$, $\Delta\omega_e$, and $\Delta\omega_h$ (the latter resulting from a fully coupled harmonic treatment) all decrease by an average of 45 cm⁻¹. The mechanical coupling, as evaluated by the quantity $\mu = \Delta\omega_h - \Delta\omega_e$, will increase the shift by an average of 25 cm⁻¹. Starting from the B3-LYP shift computed with the smaller basis set S ($\Delta\omega_{01}^{\text{B3-LYP}}(S)$), a better estimate can then be computed:

$$\Delta\omega_{01}^{\text{B3-LYP}}(L;\mu) = \Delta\omega_{01}^{\text{B3-LYP}}(S) + \delta^{\text{B3-LYP}}(L-S) + \mu \quad (5)$$

If this procedure is applied as such to the $\Delta\omega_{01}^{\text{B3-LYP}}(S)$ value for EDLxS1/NH₃, a value of $\Delta\omega_{01}^{\text{B3-LYP}}(L;\mu) = -715$ cm⁻¹ results.

The last line of Table 4 gives ϵ_L , the difference between MP2 and B3-LYP results for SIL/NH₃, both computed with the largest

basis set *L*. The B3-LYP shifts are overestimated by about 22 cm⁻¹ with respect to the MP2 ones, and if the correction term ϵ_L is taken into account, a value of $\Delta\omega_{01}^{\text{B3LYP}}(L;\mu;\epsilon_L) = -693$ cm⁻¹ is reached.

The role of the BSSE on the OH frequency shift has not been addressed here. Silvi et al.⁴⁶ have recently estimated that the BSSE artificially increases the $\Delta\omega_{01}^{\text{B3LYP}}$ shift by a constant amount of about 30 cm⁻¹. This further correction, if applied to our best $\Delta\omega_{01}^{\text{B3LYP}}(L;\mu;\epsilon_L)$ value, gives a final datum of -663 cm⁻¹.

4.4. Comparison between Cluster and Periodic Results.

The comparison between results computed for EDLxS1 and those for the cluster model A reveals the following: (1) The NH₃ molecule is bent toward the surface with a significant deviation from the linear approach to the OH group. (2) The ΔE value is considerably higher. (3) The $\Delta\omega_{01}$ is smaller. All this evidence is less marked at the HF level, even it parallels the B3-LYP results.

A more careful look at the optimized structure of EDLxS1/NH₃ reveals that a secondary weak interaction is taking place between NH₃ and the oxygen atom of the hydroxyl group belonging to the nearby crystal cell. This interaction implies that cooperative effects among hydroxyl groups are in place because the NH₃ molecule gives rise to infinitely long H-bonded chains of the kind ...OH...NH₃...OH...NH₃...OH... It has been shown⁵¹ on H-bonded clusters that the B3-LYP method overestimates cooperative effects with respect to both HF and MP2, which explains why B3-LYP results are more affected by the many body contributions than HF results. This is particularly serious for relatively poor basis sets such as those used here for geometry optimization. The behavior of such results for EDLxS1/NH₃ is highlighted by consideration of two linear correlations which hold for hydrogen-bonded systems. The first one correlates the binding energy ΔE with the intermolecular distance, H...N (Figure 3(a)). The second one, proposed by Hair and Hertl⁵² for hydrogen-bonded molecules on silica surfaces, correlates $(\Delta\omega_{01}(\text{OH})/\omega_{01}(\text{OH}))^{1/2}$ with ΔE , and is shown in Figure 3(b).

Figure 3(a) clearly shows that the secondary weak interaction is basically absent at the HF level, the H...N bond length decreasing monotonically with the increase of ΔE , at variance with the B3-LYP data for the EDLxS1/NH₃ case. Figure 3(b), however, shows a clear deviation of both the HF and the B3-LYP data sets from the Hair and Hertl correlation: clearly the $\Delta\omega_{01}$ shift is a more adequate observable than the H...N distance to spot cooperative effects in H-bonded structures. To shed further light on those interactions, we carried out a series of calculations at the B3-LYP level only on EDLxS1/NH₃ by adopting a 2 × 1 supercell (see Figure 4(a) for reference to the original cell), i.e., by doubling the size of the cell along the *z* direction, but leaving only one NH₃ molecule per unit cell (see Figure 4(b)). As a further step, the free OH group is then replaced by a H atom, as shown in Figure 4(c). At this stage, the geometries of the new structures are not optimized. In structure 4(b), the cooperative effects have been eliminated by breaking the infinite chain of NH₃ molecules, whereas in structure 4(c) the secondary weak interaction also has been dropped. The computed ΔE (ΔE^C) decreases from the former value of 59.1 (50.1) kJ/mol for structure 4(a) (see Table 1), to 53.1 (47.5) kJ/mol for structure 4(b), to 50.9 (46.0) kJ/mol for structure 4(c). From the BSSE corrected data, it turns out that 1.5 kJ/mol is due to the weak interaction, whereas cooperative effects amount to an extra 2.5 kJ/mol of the total ΔE^C of 50.1 kJ/mol for structure 4(a).

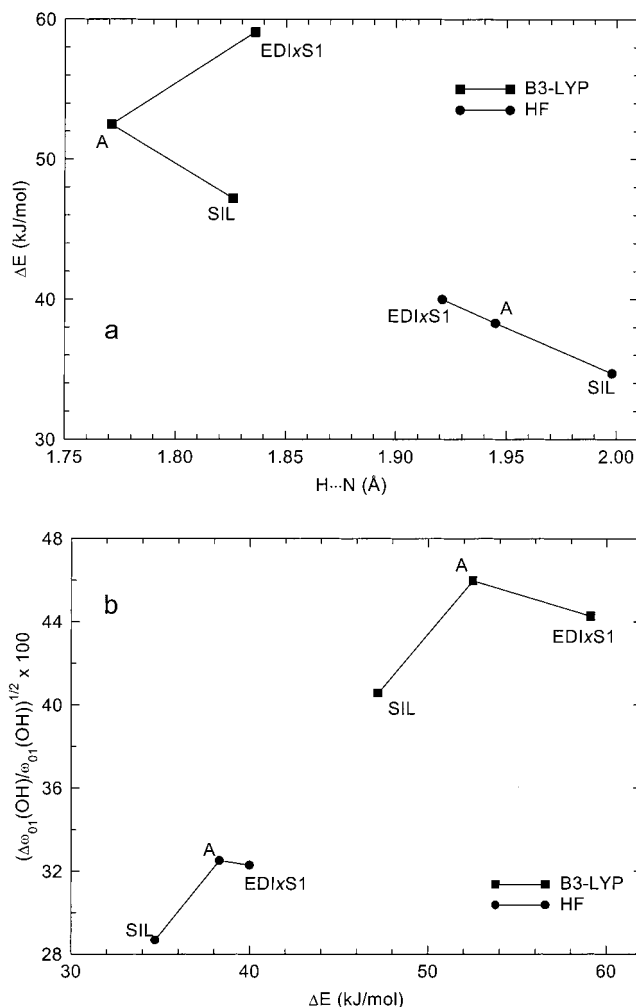


Figure 3. Section (a), Correlation between ΔE and N...H; section (b), Hair and Hertl correlation between $(\Delta\omega_{01}(\text{OH})/\omega_{01}(\text{OH}))^{1/2} \times 100$ and ΔE . Data at HF and B3-LYP levels.

As a further step, the geometry of the OH...NH₃ moiety in structure 4(c) and the corresponding anharmonic OH stretching frequency have been recomputed. The intermolecular H...N distance shortens to 1.798 Å, whereas the angles $\angle\text{O}-\text{H}\cdots\text{N}$ and $\angle\text{H}\cdots\text{N}-\text{H}$ become 178° and 109.6°, respectively, which are significantly different from the corresponding values computed for the original structure 4(a) of 1.836 Å, 174.2°, and 125.0°, respectively. As clearly appears from data in Table 1, the reoptimized EDLxS1/NH₃ structure closely resembles the cluster structure A/NH₃, even if with a noticeably longer H...N distance for the former. The binding energy ΔE (ΔE^C) is now 51.7 (46.8) kJ/mol, in close agreement with that computed for the A/NH₃ structure (see Table 1).

The corresponding $\Delta\omega_{01}(\text{OH})$ shift is -705 cm⁻¹ definitely lower than the values of -733 cm⁻¹ for EDLxS1/NH₃ and -792 cm⁻¹ for A/NH₃ (see Table 1). This last result is puzzling when we consider the similarity of both structural and energetic features between the reoptimized structure 4(c) and the A/NH₃ cluster. One obvious point is that the response of an infinite slab to a perturbation induced by ad-molecules is different from that of a cluster, even when it is structurally similar to the periodic site, as in the present case.

When comparing results within the same periodic model, we find that about 30 cm⁻¹ and 3.2 kJ/mol of the values computed for EDLxS1/NH₃ are lost in the reoptimized structure 4(c) as a consequence of the missing cooperativity and secondary interaction. From these data it can be concluded that a cagelike cluster,

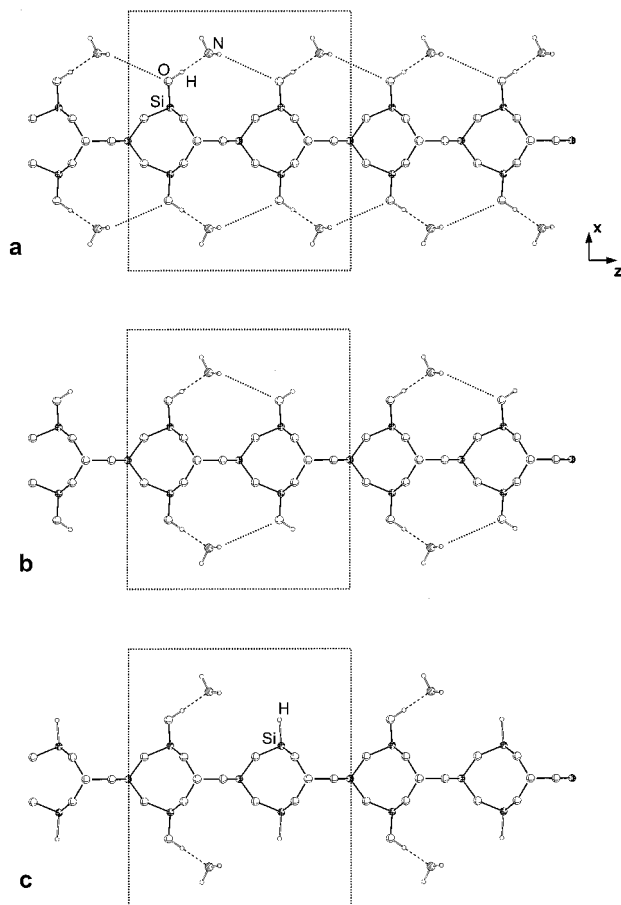


Figure 4. Supercell (2×1) for the EDLxS1/NH₃ system: section (a), original cell with one NH₃ molecule per adsorption site; section (b), cell with one NH₃ molecule and two adsorption sites; section (c), cell with one NH₃ molecule and one adsorption site (Si-H distance fixed to 1.46 Å).

when designed to fit the structural and electrical features of the active site belonging to an infinite extended surface, gives results in close agreement with those computed for the periodic system. As has been shown here, the differences between the two approaches are due mainly to supplementary weak interactions taking place between the ad-molecule and the extended surface, as well as to long-range effects not accounted for by the finite cluster.

5. Conclusions

In this work, we have used the (100) hydroxylated surface of silica edingtonite to mimic the surface of amorphous silica. The resulting OH density of the present model (around 2 OH per nm²) matches that of a highly dehydrated amorphous silica sample, as it is the computed fundamental OH stretching frequency of the isolated site. An ab initio all-electron periodic approach based on a localized Gaussian basis set has been adopted to simulate the adsorption process of the NH₃ molecule. The results have been compared with similar calculations based on well-designed molecular clusters. Moreover, comparison with the available experimental data has also been addressed for what concern both heat of adsorption and vibrational features of the surface sites. A number of conclusions can be derived from the results of this work, as follows:

(1) The interaction with NH₃ has been studied by optimizing the OH...NH₃ moiety belonging to the EDLxS1/NH₃ system with a basis set of 6-31G(d,p) quality. Comparison with similar calculations on molecular clusters SIL and A shows different

trends at the HF and B3-LYP levels, the latter showing the greatest discrepancies.

(2) The dependence of the binding energy on BSSE and quality of the basis set has been studied in great detail by use of a combination of six basis sets for the OH...NH₃ moiety and three basis sets for the framework atoms. Our B3-LYP best estimate of the heat of adsorption of NH₃ on EDLxS1 is -31.2 ± 0.6 kJ/mol, compared with the experimental molar heat of adsorption of about -45 kJ/mol and the isosteric heat of -37 kJ/mol. It is worth noting that even if it is underestimated, the result of the periodic calculation is closer to the experimental datum than the corresponding values for SIL (-21.4 ± 0.3 kJ/mol) and A (-24.5 ± 0.7 kJ/mol). BSSE correction is sizable, at around 15% of the B3-LYP binding energy.

(3) B3-LYP results definitely show that the NH₃ molecule is engaged with the nearby OH group via a weak secondary interaction which also causes the formation of an infinite long chain of H-bonded interactions. By a number of supplementary calculations, it has been shown that the weak interaction accounts for 1.5 kJ/mol and the cooperative effect for 2.5 kJ/mol of the total binding energy ΔE^C of 50.1 kJ/mol. The binding energy of a modified periodic slab EDLxS1/NH₃ in which those contributions have been selectively eliminated is 46.0 kJ/mol, very close to the value of 45.2 kJ/mol computed for cluster A.

(4) The best B3-LYP computed value of the OH frequency shifts caused by the interaction with NH₃ is -663 cm⁻¹, which includes an estimate of corrections for basis-set deficiencies, electron correlation, mechanical coupling, and BSSE. This value should be compared with the experimental datum of -950 cm⁻¹ measured on amorphous silica at 4 K.

(5) Electron correlation is essential for accurate estimation of both binding energies and OH frequency shifts, the B3-LYP values being, respectively, 56% and 70% higher than the corresponding HF values.

From points (2) and (3), it can be concluded that the computed results for the periodic model are definitely underestimated with respect to the available experimental data. Possible reasons may be the structural differences between the real surface of the amorphous silica and the proposed model derived from edingtonite, as well as the intrinsic inability of the B3-LYP method to take dispersive forces into proper account.^{53,54} This last contribution is of an attractive nature and may, when properly accounted for, improve both the heat of adsorption and the OH frequency shift.

In conclusion, the proposed periodic model of the hydroxylated (100) edingtonite surface can be profitably adopted to study adsorption processes taking place at the surface of siliceous materials, as it is a computationally appealing alternative to the cluster models of cagelike topology. These latter are indeed good models, highlighting the local nature of processes in which H-bonding interaction is the dominant component of the adsorption. In this respect, encouraging results have also been obtained in this laboratory for the cases of CO and H₂O adsorption.

Acknowledgment. The present work is part of a project coordinated by A. Zecchina and cofinanced by the Italian MURST (Cofin98, Area 03). Computer facilities from CINECA are kindly acknowledged. The authors are grateful to J. Gale for providing the most recent version of the GULP code.

References and Notes

- (1) Iler, R.K. *The Chemistry of Silica*; Wiley-Interscience: New York, 1979.
- (2) Zachariasen, W. H. *J. Am. Chem. Soc.* **1932**, *54*, 3841.

- (3) Scott, R. P. W. *Silica Gel and Bonded Phases*; John Wiley & Sons: Chichester, U.K., 1993.
- (4) Wright, A. C. *J. Non-Cryst. Solids* **1994**, 179, 84.
- (5) Garofalini, S. H. *J. Chem. Phys.* **1983**, 78, 2069.
- (6) Blonski, S.; Garofalini, S. H. *J. Am. Ceram. Soc.* **1997**, 80, 1997.
- (7) Bakaev, V. A.; Steele, W. A. *J. Chem. Phys.* **1999**, 111, 9803.
- (8) *The Surface Properties of Silicas*; Legrand, A. P.; Ed.; John Wiley & Sons: Chichester, U.K., 1998.
- (9) Knözinger, H. In *The Hydrogen Bond*; Schuster, P., Zundel, G., Sandorfy, C., Eds.; North-Holland: Amsterdam, 1976; Vol III, Chapter 27, p 1263; and reference therein.
- (10) Curthoys, G.; Davydov, V. Ya; Kiselev, A. V.; Kiselev, S. A.; Kuznetsov, B. V. *J. Colloid Interface Sci.* **1974**, 48, 58.
- (11) Morrow, B. A.; McFarlan, A. J. *J. Phys. Chem.* **1992**, 96, 1395.
- (12) Liu, C. C.; Maciel, G. E. *J. Am. Chem. Soc.* **1996**, 118, 401.
- (13) Fubini, B.; Bolis, V.; Cavenago, A.; Garrone, E.; Ugliengo, P. *Langmuir* **1993**, 9, 2712.
- (14) Sauer, J.; Ugliengo, P.; Garrone, E.; Saunders, V. R. *Chem. Rev.* **1994**, 94, 2095.
- (15) Sauer, J. *Chem. Rev.* **1989**, 89, 199.
- (16) Samthein, J.; Pasquarello, A.; Car, R. *Phys. Rev. B* **1995**, 52, 12690.
- (17) Civalieri, B.; Casassa, S.; Garrone, E.; Pisani, C.; Ugliengo, P. *J. Phys. Chem. B* **1999**, 103, 2165.
- (18) Civalieri, B.; Garrone, E.; Ugliengo, P. *Langmuir* **1999**, 15, 5829.
- (19) Meier, W. M.; Olson, D. H. *Atlas of Zeolite Structure Types*; Butterworth: London, 1987.
- (20) Sauer, J.; Ahlrichs, R. *J. Chem. Phys.* **1990**, 93, 2575.
- (21) Ugliengo, P.; Saunders, V. R.; Garrone, E. *J. Phys. Chem.* **1990**, 94, 2260.
- (22) Senchenya, I. N.; Garrone, E.; Ugliengo, P. *J. Mol. Struct. (THEOCHEM)* **1997**, 368, 93.
- (23) Garrone, E.; Kazansky, V. B.; Kustov, L. M.; Sauer, J.; Senchenya, I. N.; Ugliengo, P. *J. Phys. Chem.* **1992**, 96, 1040.
- (24) Nicholas, J. B.; Feyereisen, M. *J. Chem. Phys.* **1995**, 103, 8031.
- (25) In the present study, model A corresponds to model 4 in ref 18.
- (26) Becke, A. D. *J. Chem. Phys.* **1993**, 98, 5648.
- (27) Lee, C.; Yang, W.; Parr, R. G. *Phys. Rev.* **1988**, B37, 785.
- (28) Frisch, M. J.; Trucks, G. W.; Schlegel, H. B.; Scuseria, G. E.; Robb, M. A.; Cheeseman, J. R.; Zakrzewski, V. G.; Montgomery, J. A.; Stratmann, R. E.; Burant, J. C.; Dapprich, S.; Millam, J. M.; Daniels, A. D.; Kudin, K. N.; Strain, M. C.; Farkas, O.; Tomasi, J.; Barone, V.; Cossi, M.; Cammi, R.; Mennucci, B.; Pomelli, C.; Adamo, C.; Clifford, S.; Ochterski, J.; Petersson, G. A.; Ayala, P. Y.; Cui, Q.; Morokuma, K.; Malik, D. K.; Rabuck, A. D.; Raghavachari, K.; Foresman, J. B.; Cioslowski, J.; Ortiz, J. V.; Baboul, G. A.; Stefanov, B. B.; Liu, G.; Liashenko, A.; Piskorz, P.; Komaromi, I.; Gomperts, R.; Martin, R. L.; Fox, D. J.; Keith, T.; Al-Laham, M. A.; Peng, C. Y.; Nanayakkara, A.; Gonzalez, C.; Challacombe, M.; Gill, P. M. W.; Johnson, B. G.; Chen, W.; Wong, M. W.; Andres, J. L.; Head-Gordon, M.; Replogle, E. S.; Pople, J. A. *Gaussian 98*, Revision A.7; Gaussian, Inc.: Pittsburgh, PA, 1998.
- (29) Pisani, C.; Dovesi, R.; Roetti, C. *Hartree-Fock Ab Initio Treatment of Crystalline Solids*. In *Lecture Notes in Chemistry*, Vol. 48; Springer: Berlin, 1988.
- (30) Dovesi, R.; Saunders, V. R.; Roetti, C.; Causà, M.; Harrison, N. M.; Orlando, R.; Zicovich-Wilson, C. M. *CRYSTAL-98 User's Manual*; Università di Torino: Torino, Italy, 1999.
- (31) Gale, J. D. *GULP (the General Utility Lattice Program)*; Royal Institution/Imperial College: London, 1992–1994.
- (32) Gale, J. D. *J. Chem. Soc., Faraday Trans.* **1997**, 93, 629.
- (33) Schröder, K.-P.; Sauer, J. *J. Phys. Chem.* **1996**, 100, 11043.
- (34) Sierka, M.; Sauer, J. *Faraday Discuss.* **1997**, 106, 41.
- (35) Civalieri, B.; Zicovich, C. M.; Ugliengo, P.; Saunders, V. R.; Dovesi, R. *Chem. Phys. Lett.* **1998**, 292, 394.
- (36) Nada, R.; Nicholas, J. B.; McCarthy, M. I.; Hess, A. C. *Int. J. Quantum Chem.* **1996**, 60, 809.
- (37) Boys, S. F.; Bernardi, F. *Mol. Phys.* **1970**, 19, 553.
- (38) Lindberg, B. *J. Chem. Phys.* **1988**, 88, 3805.
- (39) Ugliengo, P. *ANHARM - A Program to Solve the Monodimensional Nuclear Schroedinger Equation*. Unpublished work, 1989.
- (40) Civalieri, B.; Garrone, E.; Ugliengo, P. *J. Mol. Struct. (THEOCHEM)* **1997**, 419, 227.
- (41) Hertl, W.; Hair, M. L. *J. Phys. Chem.* **1968**, 72, 4676.
- (42) Del Bene, J.; Person, W. B.; Szczepaniak, K. *J. Phys. Chem.* **1995**, 99, 10705.
- (43) Brändle, M.; Sauer, J. *J. Am. Chem. Soc.* **1998**, 120, 1556.
- (44) Sandorfy, C. In *The Hydrogen Bond*; Schuster, P., Zundel, G., Sandorfy, C., Eds.; North-Holland: Amsterdam, 1976; pp 613–645.
- (45) Civalieri, B.; Garrone, E.; Ugliengo, P. *J. Phys. Chem. B* **1998**, 102, 2373.
- (46) Silvi, B.; Wieczorek, R.; Latajka, Z.; Alikhani, M. E.; Dkhissi, A.; Bouteiller, Y. *J. Chem. Phys.* **1999**, 111, 6671.
- (47) Sauer, J.; Bleiber, A. *Pol. J. Chem.* **1998**, 72, 1524.
- (48) Vener, V. M.; Sauer, J. *Chem. Phys. Lett.* **1999**, 312, 591.
- (49) Jeanvoine, Y.; Ángyán, J.; Kresse, G.; Hafner, J. *J. Phys. Chem. B* **1998**, 102, 5573.
- (50) Tsiganenko, A. A.; Babaeva, M. A. *Opt. Spektrosk.* **1983**, 54, 665.
- (51) Ugliengo, P.; Ferrari, A. M.; Civalieri, B.; Garrone, E. Unpublished work, 1997.
- (52) Hair, M. L.; Hertl, W. *J. Phys. Chem.* **1970**, 74, 91.
- (53) Kristyan, S.; Pulay, P. *Chem. Phys. Lett.* **1994**, 229, 175.
- (54) Perez-Jorda, J.-M.; Becke, A. D. *Chem. Phys. Lett.* **1995**, 229, 134.